Acta Pharmacologica Sinica

www.nature.com/aps

ARTICLE

Selective EZH2 inhibitor zld1039 alleviates inflammation in cisplatin-induced acute kidney injury partially by enhancing RKIP and suppressing NF-κB p65 pathway

Li Wen[1], Shao-hua Tao[1], Fan Guo[1], Ling-zhi Li[1], Hong-liu Yang[1], Yan Liang[2], Li-dan Zhang[3], Liang Ma[1] and Ping Fu[1]

Enhancer of zeste homolog 2 (EZH2), a component of polycomb repressive complex 2 (PRC2), is a histone lysine methyltransferase mediating trimethylation of histone H3 at lysine 27 (H3K27me3), which is a repressive marker at the transcriptional level. EZH2 sustains normal renal function and its overexpression has bad properties. Inhibition of EZH2 overexpression exerts protective effect against acute kidney injury (AKI). A small-molecule compound zld1039 has been developed as an efficient and selective EZH2 inhibitor. In this study, we evaluated the efficacy of zld1039 in the treatment of cisplatin-induced AKI in mice. Before injection of cisplatin (20 mg/kg, i.p.), mice were administered zld1039 (100, 200 mg/kg, i.g.) once, then in the following 3 days. We found that cisplatin-treated mice displayed serious AKI symptoms, evidenced by kidney dysfunction and kidney histological injury, accompanied by EZH2 upregulation in the nucleus of renal tubular epithelial cells. Administration of zld1039 dose-dependently alleviated renal dysfunction as well as the histological injury, inflammation and cell apoptosis in cisplatin-treated mice. We revealed that zld1039 administration exerted an anti-inflammatory effect in kidney of cisplatin-treated mice via H3K27me3 inhibition, raf kinase inhibitor protein (RKIP) upregulation and NF-κB p65 repression. In the cisplatin-treated mouse renal tubular epithelial (TCMK-1) cells, silencing of RKIP with siRNA did not abolish the anti-inflammatory effect of EZH2 inhibition, suggesting that RKIP was partially involved in the anti-inflammatory effect of zld1039. Collectively, EZH2 inhibition alleviates inflammation in cisplatin-induced mouse AKI via upregulating RKIP and blocking NF-κB p65 signaling in cisplatin-induced AKI. The potent and selective EZH2 inhibitor zld1039 has the potential as a promising agent for the treatment of AKI.

Keywords: acute kidney injury; inflammation; enhancer of zeste homolog 2; Raf kinase inhibitor protein; NF-κB p65; zld1039

Acta Pharmacologica Sinica (2022) 43:2067–2080; https://doi.org/10.1038/s41401-021-00837-8

INTRODUCTION

Acute kidney injury (AKI) is a familiar clinical disease, and there has been a high morbidity and mortality, accounting for approximately 1.7 million deaths per year [1, 2]. A rapid decline in glomerular filtration rate is an essential characteristic of AKI [3]. AKI is predisposed to occur and develop to chronic kidney disease (CKD) or end-stage renal disease [4]. Commonly, AKI is caused by diverse pathological conditions, including trauma, sepsis, ischemia, and nephrotoxic agents, especially cisplatin (dichlorodiamino platinum) [5, 6]. The cisplatin-based anti-tumor effect has been widely used for clinical chemotherapy [7]. Unfortunately, about one-third of cisplatin chemotherapy patients may occur AKI [8]. To date, there is no valid strategy for preventing or improving cisplatin-induced AKI. Hence, it is urgent to explore novel and effective drug candidate to protect against cisplatin nephrotoxicity.

Generally, cisplatin is mainly absorbed and aggregated by the proximal tubular cells through organic cation transporter, which is located on the basolateral side of the tubular cells. Thus, it has less impact on the glomerular and distal tubule [9, 10]. Increased cisplatin concentration in proximal renal tubule leads to forming platinum complexes that could trigger multiple signaling pathways, resulting in DNA damage, autophagy inhibition, inflammatory response, and apoptosis [11, 12].

Recently, studies have reported that epigenetics, especially histone methylation, which is catalyzed by histone lysine and arginine methyltransferases, is closely involved in the development and progression of AKI [13, 14]. Enhancer of zeste homolog 2 (EZH2), a component of polycomb repressive complex 2 (PRC2), is a histone lysine methyltransferase. EZH2 not only sustains normal kidney physiology, but also impedes the expression of protective genes to facilitate AKI progression by mediating trimethylation of histone H3 at lysine 27 (H3K27me3), which is a repressive marker at the transcriptional level [13, 15]. In the ischemia-reperfusion (I/R) or folic acid (FA) induced AKI mice, EZH2 was upregulated and it reduced the expression of E-cadherin and ZO-1, leading to the disruption of epithelial adhesion and barrier function [13]. Given that EZH2 has a PRC2-independent function, and it could also activate transcription. Considerable studies have been conducted to explore the transcriptional activation role of EZH2 [16, 17]. For

[1]Kidney Research Institute, National Clinical Research Center for Geriatrics and Division of Nephrology, West China Hospital of Sichuan University, Chengdu 610041, China; [2]Research Core Facility of West China Hospital, Chengdu 610041, China and [3]Laboratory of Anesthesia & Critical Care Medicine, Translational Neuroscience Center, West China Hospital of Sichuan University, Chengdu 610041, China
Correspondence: Li-dan Zhang (zhanglidan0510@wchscu.cn) or Liang Ma (liang_m@scu.edu.cn)

Received: 27 September 2021 Accepted: 1 December 2021
Published online: 22 December 2021

example, EZH2 has been shown to activate androgen receptor (AR), to regulate AR gene transcription and it facilitates prostate cancer progression [18]. Several researchers have identified the intimate links between EZH2 and cancers, such as breast cancer [19], prostate cancer [20], melanoma [21], and bladder cancer [22], etc. EZH2 has also been demonstrated to be related to kidney damage, including ischemia-reperfusion injury [13], renal fibrogenesis [23], renal tubular cell apoptosis [14], and hyperuricemia-induced CKD [24]. The zld1039 (Fig. 1a) is an efficient and highly selective EZH2 small-molecule inhibitor, and it could induce tumor cell cycle arrest and apoptosis, as well as inhibit tumor growth [25]. However, the role of zld1039 as a drug candidate by inhibiting EZH2 for AKI treatment is not clear. For these reasons, we hypothesized that zld1039 treatment alleviated AKI inflammation by inhibiting EZH2. Thus, in this study, we wanted to investigate the protective effect of zld1039 on AKI and its specific mechanism.

MATERIALS AND METHODS

Agents, antibodies, and primer sequences

Cisplatin was purchased from Synguider (CAS: 15663-27-1; Chengdu, China). zld1039 was given by the State Key of Laboratory of Biotherapy, Sichuan University (Sichuan, China). Antibodies and primer sequences were displayed in Tables S1 and S2.

Animals and experiments design

Male C57BL/6J mice (8–10 weeks, 23–25 g) were obtained from the Animal Laboratory Center of Sichuan University (Chengdu, China). The mice were kept in a controlled environment (temperature at 22 ± 2 °C and 12:12 h light/dark conditions). Food and water were supplied optionally. After 1 week of adaptive feeding, the mice were randomly divided into five groups: control group ($n = 6$), zld1039 (200 mg/kg) group ($n = 4$), cisplatin (cis) group ($n = 8$), cis + zld1039 (100 mg/kg) ($n = 8$), cis+zld1039 (200 mg/kg) ($n = 8$). All the experimental procedures were authorized by the Animal Care and Use Ethics Committee of Sichuan University (2020205A).

To establish the cisplatin-induced mouse AKI model, cisplatin (20 mg/kg) was dissolved in 100 μL 0.9% saline for intraperitoneal (i.p.) injection. zld10039 was also dissolved in 100 μL 0.9% saline and prepared into suspension after 37 °C ultrasonic treatments for oral administration. zld1039 (100, 200 mg/kg) was given orally to mice 1 h before cisplatin administration on d 1. Then, it was administered daily for three consecutive days. The control group was injected and gavaged with an equal volume of 0.9% saline. The mice in the zld1039 group were only administered orally 200 mg/kg zld1039 for three consecutive days to determine whether it has toxic and limiting side effects. All mice were euthanized with chloral hydrate (3 mL/kg, i.p.) 72 h after cisplatin injection. Kidney tissues were harvested for histologic examination, and they were stored at −80 °C for mRNA and protein analysis. Serum was taken to measure serum creatinine (Scr) and blood urea nitrogen (BUN).

Serum biochemistry assay

The serum was centrifuged at 3000 × *g* for 15 min, and the supernatant was taken to detect Scr and BUN by an automatic biochemical analyzer (Mindray BS-240). When the Scr levels in the cisplatin group were two times higher than that in the control group, the cisplatin-induced mouse AKI model was thought to be successfully established.

Pathological evaluation

Renal tissues were fixed with 10% phosphate-buffered formalin and then embedded in paraffin. Paraffin sections (4 μm) were deparaffinized, rehydrated, washed and then used for Hematoxylin-Eosin (H&E) and Periodic Acid-Schiff (PAS) staining. Tubular dilation, brush border disappears, cast formation, and tubular epithelial cell necrosis and detachment were used to semi-quantitatively score renal tubular damage. The detailed scoring criteria were as follows: the scores of renal tubular injury ranged from 0–4, 0 = 0%, 1 = 1%–25%, 2 = 26%–50%, 3 = 51%–75%, 4 ≥ 76%, respectively. Ten consecutive fields of ×20 magnification were selected from three samples in each group for scoring, and the average was taken.

Immunohistochemistry and immunofluorescence staining

Paraffin sections (4 μm) were first deparaffinized and restored antigen and then blocked with 1× horse serum. Primary antibodies were incubated overnight at 4 °C. The sections were washed thrice in phosphate-buffered saline (PBS), and the corresponding secondary antibodies were incubated for 1 h at room temperature. Immunofluorescence secondary antibodies were naturally fluorescent. Next, after washing with PBS, the sections were stained with DAPI (D8200; Solarbio) and sealed with 50% glycerin. ZEN 2012 microscopy software was used to photo collecting.

TUNEL staining

The terminal deoxynucleotidyl transferase-mediated dUTP nick end labeling (TUNEL) staining was performed to detect kidney tissue cell apoptosis. TUNEL-positive cells were shown in brown. The images were taken with upright microscopy at ×200 or ×400 original magnifications. Then, we used Image Pro-Plus Software (Media-Cybernetics, Silver Spring, MD) to quantitatively evaluate the TUNEL-positive staining areas. Three sections for each group were selected, and at least ten fields (magnification ×200) per section was calculated, and the average ratio was taken to a graph.

CHIP assay

According to the manufacturer's instructions, the CHIP Assay Kit (Millipore, MA, USA) was used to detect the physically binding of proteins and DNA promoter regions. CHIP antibodies (Table S1) and the primers used for CHIP (Table S2) were displayed. The precipitated DNA fragments were quantified by quantitative real-time polymerase chain reaction (qRT-PCR), and the CQ value of input was used as an internal reference control. The enrichment efficiency of CHIP-qPCR was presented by the relative enrichment ratio of input signal: calculation of CHIP signal (%input) = 2 (−ΔCt [normalized ChIP]) × 100%, ΔCt [normalized ChIP] = Ct [ChIP] − (Ct [Input] − Log2 (Input Dilution Factor)), Input Dilution Factor = 100.

Cell culture and treatment

Mouse renal tubular epithelial cells (TCMK-1) were cultured in an environment of 5% CO_2—95% air at 37 °C. The MEM medium (G4550-500ML, Sercicebio) containing 10% fetal bovine serum (FBS) (SH30084.03, Hyclone) was used to culture TCMK-1 cells. The resuscitated cells usually reproduced for two generations before formal experiments began. Then, TCMK-1 cells were plated in 6-well culture plates at 8×10^4 cells per well. TCMK-1 cells density reached 50%–60%, and they were starved in 0.5% FBS medium for 6 h. The cells were randomly divided into six groups: control group, zld1039 group (1.6 μM), cis group (10 μg/mL), cis + zld1039 group (0.4 μM, 0.8 μM, 1.6 μM). zld1039 was incubated simultaneously with cisplatin (the concentration of zld1039 was selected by the results of CCK8 assay). After 24 h with or without the zld1039 treatment, the cells were harvested for qRT-PCR and Western blot (WB) analysis.

CCK8 assay

The CCK8 kit was used to detect cell viability. First, 5×10^3 TCMK-1 cells were seeded in 96-well plates. After 6 h of starvation, the zld1039 at different concentrations was added in the culture

medium with or without cisplatin (10 μg/mL) for 24 h. The original culture medium was suck out, and the new culture medium (100 μL) containing CCK8 solution (10 μL) was added and incubated for 1 h. The culture medium gradually turned yellow and the absorbance at 450 nm was determined by a microplate reader.

Flow cytometry assay
Cell apoptosis was evaluated by the Annexin V-FITC apoptosis analysis kit (AO2001-02P-H, SUNGENE). The 1×10^4 TCMK-1 cells were seeded in 12-well plates. After 6 h of starvation, cisplatin or zld1039 were given according to the above groups. The supernatant was collected after 24 h. Adhered cells were washed once with 200 μL PBS, and were digested by trypsin. The cells were centrifuged at 2000 r/min for 5 min, and the cell precipitation was collected. The cells were resuspended with 1 mL PBS and centrifuged again. Then, the cells were resuspended with 100 μL 1× buffer and 5 μL Annexin V-FITC, and 5 μL propidium (PI) was stained in the dark for 10 min. Cell apoptosis was detected by flow cytometry (BD Biosciences, AccuriC6, USA). The quadrant diagram represents the results as follows: mechanically damaged cells (Annexin V^+/PI^-), necrotic or late apoptotic cells (Annexin V^+/PI^+), viable apoptotic cells (Annexin V^-/PI^+) and intact cells (Annexin V^-/PI^-).

Transfection of siRNA
The small interfering RNA (siRNA) oligonucleotides specifically targeting mouse RKIP were designed to knockdown RKIP. When the cells density reached 30%–40% in an antibiotic-free culture medium, they were transfected with RKIP-siRNA (50 nM) with riboFECT™ CP transfection reagent (Guangzhou, China) in 0.5% FBS culture medium. The NC-siRNA (50 nM) was used as a negative control. The transfection procedure is detailed in the instructions. The cells were transfected for 24 h, and were exposed to cisplatin (10 μg/mL) in the presence or absence of zld1039 (1.6 μM) for an additional 24 h. The RKIP-siRNA sequences were displayed in Table S2.

Western blot analysis
Radio immune precipitation lysis buffer (P0013B, Beyotime Biotechnology) containing 1‰ proteinase inhibitors (Keygen Biotech) was used to homogenize kidney tissues or TCMK-1 cells. The lysate was centrifugated at 13,000 × *g* for 15 min at 4 °C. Bovine albumin was used as the standard. The Pierce™ BCA Protein Assay Kit (23225; Thermo Scientific) was used to measure the protein concentrations. According to the different molecular weight of protein, 10%–12% SDS-PAGE gels were selected to separate proteins. Then, the gels were transferred onto polyvinylidene difluoride membrane (Bio-Rad), and 5% non-fat milk was used as blocking reagent. The membranes were incubated with corresponding primary antibodies overnight at 4 °C. Tris-buffered saline-Tween washed thrice, and the horseradish peroxidase-conjugated secondary antibodies were used. Bound antibodies were displayed by the Immobilon Western Chemiluminescent HRP Substrate (WBKLS0500; Millipore Corporation) with Bio-Rad Chemi Doc MP. ImageJ 6.0 software (National Institutes of Health) was used to analyze gray value. GAPDH was used as an internal control to normalize the gray density of protein bands. All immunoblot analysis data were obtained from triplicate experiments.

RNA extraction, cDNA synthesis, and qRT-PCR
Total RNA was isolated by Animal Total RNA Isolation Kit (Foregene, Cheng, China). The cDNA was produced by 1 μg RNA according to the HiScript® III RT SuperMix for qPCR (+gDNA wiper) (Vazyme, Nanjing, China). In brief, the RNA was incubated with 4 μL 4× gDNA wiper Mix at 42 °C for 2 min and then 4 μL 5× Hiscript III qRT SuperMix was added. The sample was mixed gently with a pipette and the reverse transcription reaction was performed under the following conditions: at 37 °C for 15 min and 85 °C for 5 s. The product could be directly used in qPCR reactions. The primers are described in Table S2.

Statistical analysis
All experiments were repeated at least three times in this study. Quantitative data involved in this study were presented as mean ± SEM. Intergroup comparisons were performed using one-way analysis of variance. Multiple means were compared by using Tukey's test, and the differences between the two groups were determined by the Student's *t* test. All statistical graphs were done by Prism 9.0 (GraphPad Software, San Diego, CA, USA). Values of $P < 0.05$ was considered statistically significant.

RESULTS

Pharmacologic EZH2 inhibition by zld1039 ameliorated renal dysfunction and histologic damage in cisplatin-induced AKI mice
First, HE staining was used to detect the toxic and side effects of zld1039 on heart, liver, spleen, and kidney, and the results showed that zld1039 had no significant effect on the corresponding organs (Fig. S1). To explore whether EZH2 inhibition by zld1039 has a protective role in cisplatin-induced AKI, we assessed renal function (Scr and BUN) and pathological changes. As shown in Fig. 1b, c, the Scr and BUN were markedly increased in the cisplatin group compared with the control group, and zld1039 alone did not increase Scr and BUN. The zld1039 dose-dependently reduced cisplatin-induced the level of Scr and BUN compared to those of the cisplatin group. Similarly, zld1039 treatment inhibited the mRNA levels of kidney injury markers havcr1 (Kim-1) and lcn2 (NGAL) in a dose-dependent manner (Fig. 1d, e). Similarly, the NGAL protein of injured kidneys was decreased after zld1039 treatment (Fig. 1f, g). The H&E and PAS staining revealed that zld1039 markedly improved pathological damage of kidney, including renal tubular dilation, cast formation, brush border disappearance, tubular epithelial cell necrosis and detachment (Fig. 1h, i). Tubular damage scores were lower in zld1039-treated AKI mice than that in the cisplatin mice (Fig. 1j).

EZH2 inhibition by zld1039 attenuated kidney inflammation and apoptosis in cisplatin-induced AKI mice
Renal inflammation is a common pathogenic denominator in cisplatin-induced kidney injury [26]. As shown in Fig. 2a–c, the mRNA levels of IL-6, IL-1β, TNF-α, and MCP-1 were enhanced in kidneys of cisplatin-induced AKI mice, but that was inhibited by zld1039. Besides, apoptosis of renal proximal tubule cell is a crucial mechanism of cisplatin-induced AKI [12]. Hence, we next evaluated the effect of zld1039 on renal tubular cells death in the kidneys of cisplatin injected mice by measurement of cleaved caspase 3 (an advancing apoptosis biomarker) and TUNEL-positive cells. The protein expression of cleaved caspase 3 was increased in the cisplatin group while it was reduced by zld1039 treatment (Fig. 2d, e). As expected, TUNEL-positive cell was not found in normal, but it was obvious in the cisplatin-injured kidney tissues. Oral administration of zld1039 markedly reduced the number of apoptotic tubular cells (Fig. 2f, g). Taken together, our results indicated that zld1039 ameliorated cisplatin-induced kidney inflammation and apoptosis in mice.

EZH2 inhibition by zld1039 suppressed H3K27me3 expression in cisplatin-induced AKI mice
Further, we examined EZH2 and H3K27me3 expression in cisplatin-induced murine kidneys. As exhibited in Fig. 3a, the immunohistochemistry staining illustrated that cisplatin increased EZH2 nuclear expression in kidney tissue. By contrast, zld1039 dramatically reduced the numbers of EZH2-positive cells. Simultaneously, zld1039 dose-dependently abated the mRNA (Fig. 3b) and protein (Fig. 3c, d) levels of EZH2 in the injured kidneys. Similar findings have emerged that zld1039 markedly reduced H3K27me3 in a dose-dependent manner, which is a most pivotal form of histone methylation of EZH2 (Fig. 3c, e). These results

implicated that zld1039 suppressed EZH2 methyltransferase activity to reduce H3K27me3 expression in cisplatin-induced AKI mice.

EZH2 inhibition by zld1039 impeded the activation of NF-κB p65 signaling in cisplatin-induced AKI mice

NF-κB p65 signaling is a canonical inflammation pathway, which contributes to renal inflammation induced by cisplatin [14]. To investigate whether EZH2 inhibition by zld1039 could impact NF-κB activation, we examined the expression of the NF-κB p65 signaling pathway in cisplatin-induced AKI. The phosphorylation levels of p65 and IκBα were increased after cisplatin injection and suppressed by zld1039 (Fig. 4a–d). Notably, the expression of total p65 was also dramatically enhanced at the transcriptional and protein levels in the cisplatin group while was attenuated by zld1039 (Fig. 4a, e, f). Thus, we speculated that EZH2 and H3K27me3 might directly regulate p65 expression by protein-DNA binding.

Based on CHIP-Atlas database, we found that p65 (Rela)-binding peaks overlap with EZH2 [27] and H3K27me3 [28]-binding peaks on the genome level (Fig. S2a, b), suggesting that EZH2 and H3K27me3 may recruit p65 (Rela) to genomic sites for transcriptional regulation. We therefore designed RKIP (pebp1) promoter primers based on overlapping peaks and used CHIP-qPCR assay in cisplatin-induced kidney tissues. First, we found that H3K27me3 was observably bound to the p65 (Rela) promoter regions, while cisplatin stimulation inhibited H3K27me3 to bind to these regions (Fig. 4g). The inhibitory effect of H3K27me3 on p65 (Rela) transcription was weakened, which may be one reason for the upregulation of NF-κB p65. However, despite repeated trials, we failed to detect the colocalization of EZH2 and Rela promoter by CHIP assay (data not shown). In addition to the H3K27me3, a repressive marker of EZH2, it has a methylation-independent function. Kim et al. found that EZH2 co-existed with H3K27ac at the AR promoter and facilitated its transcription [18]. As expected, cisplatin increased H3K27ac expression accompanied by EZH2 upregulation, and EZH2 inhibition by zld1039 reduced H3K27ac protein level (Fig. S3). These results indicated that H3K27ac might promote NF-κB p65 expression by co-existing with EZH2. It is unknown how H3K27ac is recruited to NF-κB p65 promoter to control its transcription through EZH2. Taken together, these data implicated that EZH2 mediated NF-κB p65 signaling pathway activation to motivate renal inflammation, and EZH2 inhibition by zld1039 blocked NF-κB p65 signaling pathway.

EZH2 inhibition by zld1039 preserved the RKIP expression in cisplatin-induced AKI mice

Raf kinase inhibitor protein (RKIP), a member of the phosphatidylethanolamine-binding protein (PEBP) family [29], is regulated by EZH2 and H3K27me3 [20] and plays a key role in translocation of NF-κB [30]. We found that RKIP was downregulated in the kidneys of cisplatin group, and EZH2 inhibitor zld1039 successfully rescued the expression of RKIP (Fig. 5a, b). Consistently, the immunofluorescence staining revealed that in the cisplatin group, RKIP in the cytoplasm of renal tubule cells was reduced, while oral administration of zld1039 increased RKIP expression (Fig. 5d). In the Gene Expression Omnibus database under accession number GSE106993 [31], the RNA-sequencing data also revealed that there was significant RKIP downregulation in the kidneys of cisplatin-stimulated mice (Fig. S4). The molecular mechanisms by which RKIP expression is downregulated during tumor progression have been elucidated. In LNCaP cells, Gang et al. discovered that after expressing wild-type EZH2 with a plasmid, the RKIP (pebp1) promoter activity was significantly inhibited in luciferase reporter assays. Moreover, they further confirmed direct binding between EZH2 and the RKIP (pebp1) promoter region using CHIP assay [20]. Thus, to explore whether EZH2 and RKIP (pebp1) promoter regions have directly physically binding, we used CHIP assay to explore protein-DNA binding in cisplatin-induced AKI mice based on the CHIP-seq overlap peaks data between RKIP (pebp1) and EZH2 (Fig. S2c) or H3K27me3 (Fig. S2d). We found that EZH2 did not directly recruit to the RKIP (pebp1) promoter (data not shown). Interestingly, H3K27me3 (a repressive marker), the main expression form of EZH2 enzymatic activity, binds to the RKIP (pebp1) promoter region. As expected, the level of H3K27me3 on the RKIP (pebp1) promoter in the kidneys of cisplatin mice was higher than that of control mice (Fig. 5c). These results indicated that inhibition of RKIP expression by EZH2 mainly depends on its methyltransferase catalytic activity, and this inhibition existed at the transcription initiation level. This is consistent with previous researches [20].

EZH2 inhibition by zld1039 alleviated cisplatin-induced mouse renal tubular epithelial cell apoptosis and inflammation

Cell viability was assessed by CCK8 assay in TCMK-1 cells. The cell viability was not affected under incubation of 0.1, 0.2, 0.4, 0.8, 1.6 μM zld1039, while cell growth was inhibited under higher concentration of 3.2 and 6.4 μM zld1039 (Fig. 6a). In cisplatin-induced TCMK-1 cells, cisplatin (10 μg/mL) repressed cell viability while zld1039 restored cell viability at 0.4, 0.8, 1.6 μM (Fig. 6b). Based on these results, 0.4, 0.8, 1.6 μM of zld1039 were used for the following experiments. Furthermore, we estimated the role of zld1039 in cisplatin-induced TCMK-1 cells apoptosis. In Fig. 6c, zld1039 markedly improved cell damage caused by cisplatin under the light microscope. Apart from that, as shown in Fig. 6d, e, cisplatin induced TCMK-1 cells apoptosis, which was markedly improved by zld1039 in a dose-dependent manner as evidenced by flow cytometry. Similarly, zld1039 decreased the cleaved caspase 3 expression in cisplatin-stimulated TCMK-1 cells (Fig. 7a, e). Furthermore, inflammatory cytokines such as IL-1β, TNFα, and IL-6 were lower in zld1039-treated TCMK-1 cells (Fig. 7a–d). These results are in accordance with our in vivo data, indicating the anti-apoptosis and anti-inflammation role of zld1039 in cisplatin-induced TCMK-1 cells.

EZH2 inhibition by zld1039 repressed cisplatin-induced mouse renal tubular epithelial cells apoptosis and inflammation in H3K27me3-dependent manner

3-DZNeP, another EZH2 inhibitor, was reported to suppress renal tubular cell apoptosis and inflammation via H3K27me3 inhibition [14]. Here, we used TCMK-1 cells to examine whether zld1039 exerts anti-apoptotic and anti-inflammatory effects by inhibition of EZH2-dependent pathway. As shown in Fig. 8a–c, the mRNA and protein levels of EZH2 were enhanced in the cisplatin group compared with that in the control group. The zld1039 treatment decreased EZH2 expression at both transcriptional and protein levels and inhibited H3K27me3 protein expression (Fig. 8b, d). Interestingly, although zld1039 alone could not inhibit the expression of EZH2, it markedly inhibited EZH2 enzyme activity, resulting in the inhibition of H3K27me3. These data implicated that zld1039 mainly contributed to inhibiting EZH2 enzyme activity, and the expression of EZH2 itself was repressed by zld1039 only when the expression of EZH2 was elevated.

EZH2 inhibition by zld1039 preserved RKIP and inhibited NF-κB p65 signaling activation in cisplatin-induced TCMK-1 cells

Given that EZH2 could repress RKIP expression through physically recruiting H3K27me3 to the RKIP (pebp1) promoter. In the cisplatin-stimulated TCMK-1 cells, exposure to cisplatin reduced RKIP expression, while zld1039 (0.8 and 1.6 μM) distinctly upregulated RKIP expression (Fig. 9a, b). RKIP could bind to IκBα and inhibit NF-κB signaling activation [30]. Consistent with our in vivo observations, zld1039 treatment restored the cisplatin-induced upregulation of p65, p-p65 and p-IκBα in TCMK-1 cells (Fig. 9a, c–f). These data further verified that EZH2 inhibition by zld1039 enhanced RKIP expression and inhibited NF-κB p65

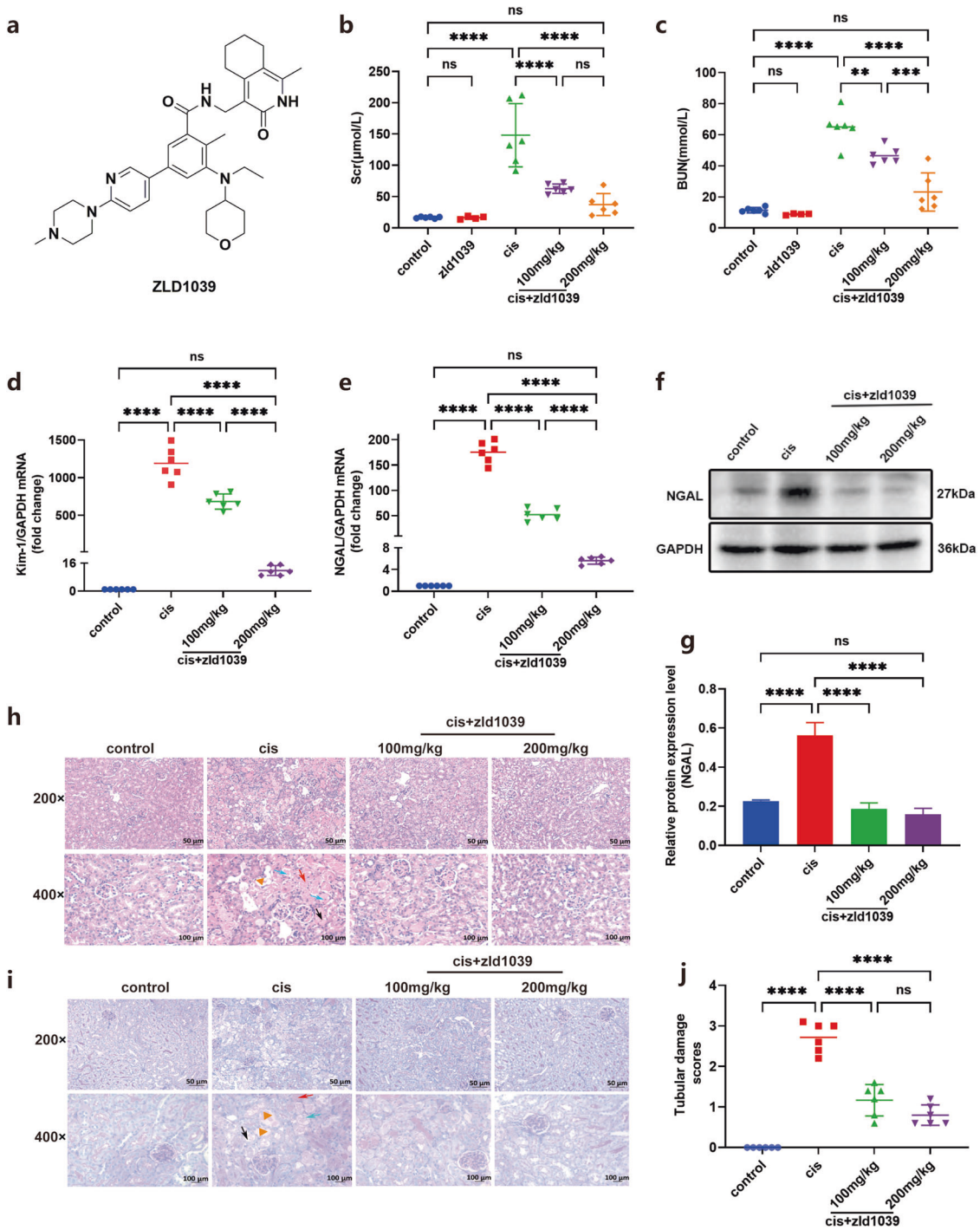

Fig. 1 EZH2 inhibition by zld1039 protected renal dysfunction and alleviated histologic damage in cisplatin-induced AKI mice. **a** Chemical structure of zld1039; **b**, **c** Scr and BUN levels ($n = 6$); **d**, **e** The mRNA levels of Kim-1 and NGAL ($n = 6$); **f**, **g** Protein expression of NGAL were quantified by densitometry and normalized with GAPDH; **h**, **i**, **j** Representative sections of H&E and PAS staining of kidney tissues (original magnification ×200 and ×400) and tubular change scores were calculated according to the criterion in materials and methods. Data are represented as means ± SDs ($n = 6$). $^{****}P < 0.0001$, $^{***}P < 0.001$, $^{**}P < 0.01$, $^{ns}P > 0.05$. All Western blot analyses were performed in two randomized mice from each group, and the experiments were repeated in triplicate.

activation, thus alleviating cell apoptosis and inflammation following cisplatin-induced AKI.

Effect of RKIP knockdown on inflammation in cisplatin-stimulated TCMK-1 cells

To demonstrate the above-mentioned results, we assessed the effect of siRNA-mediated RKIP silencing on cisplatin-induced inflammation in TCMK-1 cells. RKIP was effectively knocked down by RKIP-siRNA, and RKIP-siRNA #2 was chosen to carry out subsequent experiments based on knockdown efficiency (Fig. 10a–c). In cisplatin-induced TCMK-1 cells, transfection of RKIP-siRNA observably increased IL-6, TNFα, and IL-1β compared with NC-siRNA (Fig. 10g–m), indicating that RKIP deficiency aggravated cisplatin-induced inflammation. Interestingly, although zld1039 did not upregulate RKIP expression

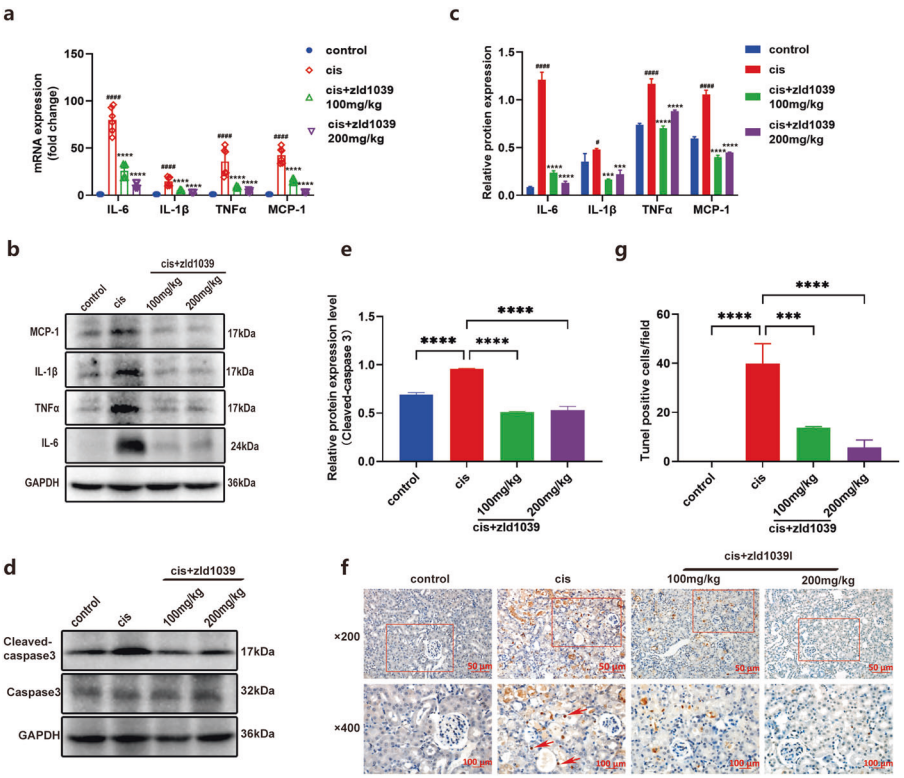

Fig. 2 EZH2 inhibition by zld1039 attenuated renal inflammation and cell apoptosis in cisplatin-induced AKI mice. a The mRNA levels of IL-6, IL-1β, TNF-α, and MCP-1 ($n = 6$); **b**, **c** Protein expression of IL-6, IL-1β, TNF-α, and MCP-1 was quantified by densitometry and normalized with GAPDH; $^{\#\#\#\#}P < 0.0001$, $^{\#}P < 0.05$ compared with the control group. $^{****}P < 0.0001$, $^{***}P < 0.001$ compared with the cis group. **d**, **e** Protein expression levels of caspase 3 and cleaved caspase 3 were quantified by densitometry and normalized with GAPDH; **f**, **g** Photomicrographs illustrating TUNEL staining of kidney tissues (magnification ×200 and ×400). The TUNEL-positive regions (brown in **f**) relative to the whole area from ten randomly cortical fields were measured. Data are represented as the means ± SDs. $^{****}P < 0.0001$, $^{***}P < 0.001$. All Western blot analyses were performed in two randomized mice from each group, and the experiments were repeated in triplicate.

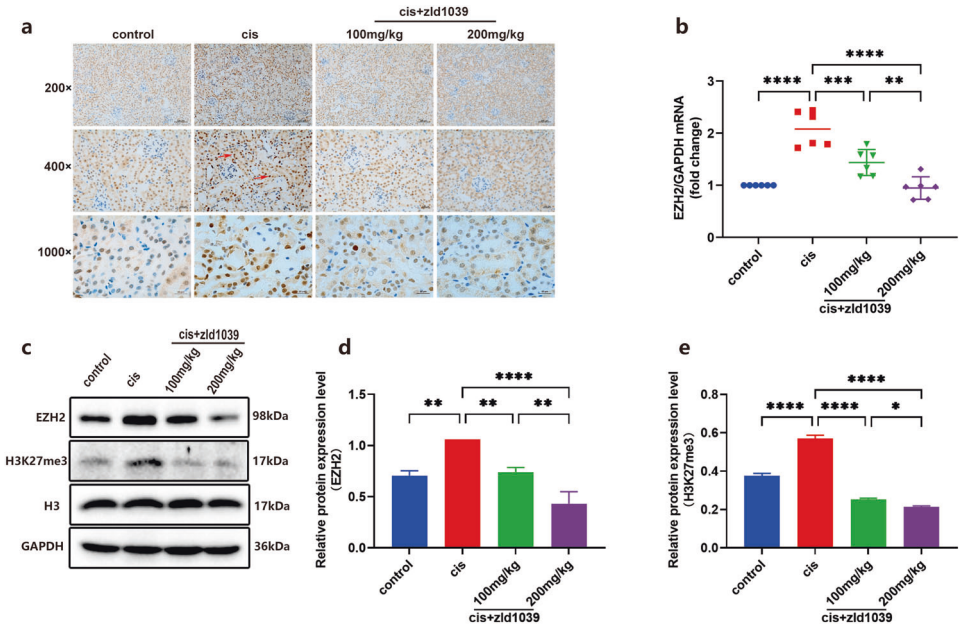

Fig. 3 EZH2 inhibition by zld1039 suppressed H3K27me3 expression in cisplatin-induced AKI mice. a Photomicrographs (×200, ×400, ×1000) illustrate EZH2 immunohistochemistry staining of kidney tissues from control or 20 mg/kg cisplatin-treated mice with/without zld1039 administration; **b** The mRNA level of EZH2 ($n = 6$); **c**–**e** Protein expression levels of EZH2 and H3K27me3 were quantified by densitometry and normalized with GAPDH. $^{****}P < 0.0001$, $^{***}P < 0.001$, $^{**}P < 0.01$, $^{*}P < 0.05$. All Western blot analyses were performed in two randomized mice from each group, and the experiments were repeated in triplicate.

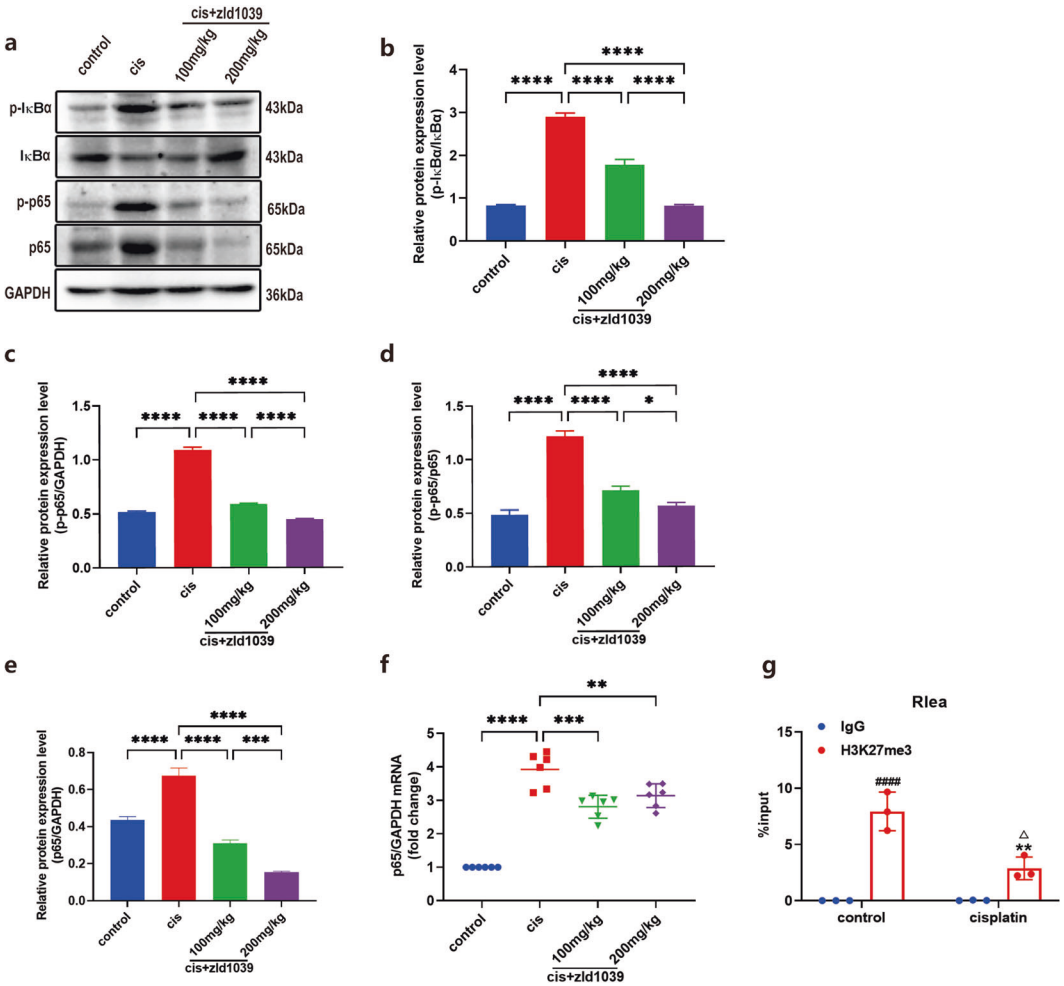

Fig. 4 EZH2 inhibition by zld1039 blocked NF-κB signaling activation in cisplatin-induced AKI mice. a–e Protein expression levels of p65, IκBα and p-p65, p-IκBα, were quantified by densitometry and normalized with GAPDH; **f** The mRNA level of p65 ($n = 6$); $^{****}P < 0.0001$, $^{***}P < 0.001$, $^{**}P < 0.01$, $^{*}P < 0.05$. **g** Control and cisplatin treated mice kidney tissues were subjected to ChIP assays using immunoglobulin G (IgG) and the H3K27me3 antibody. The amounts of precipitated p65 (RIea) DNA were quantified by qPCR using primers amplifying the regions indicated in Table S2. The data are presented as mean ± SD ($n = 3$). $^{\#\#\#\#}P < 0.0001$ compared with the control group IgG. $^{**}P < 0.01$ compared with the cisplatin group IgG antibody. $^{\triangle}P < 0.05$ compared with the control group H3K27me3 antibody. All Western blot analyses were performed in two randomized mice from each group, and the experiments were repeated in triplicate.

(Fig. 10d–f), it reduced IL-6, TNFα, and IL-1β levels (Fig. 10g–m). These results demonstrated that the upregulation of RKIP is not necessary for zld1039 to exert anti-inflammatory effect.

To confirm the role of RKIP in the NF-κB signaling in cisplatin-induced TCMK-1 cells, RKIP-siRNA #2 was transfected, and the p65, p-p65, and p-IκBα were obviously increased following cisplatin stimulation compared with NC-siRNA. However, the p65 and p-p65, rather than p-IκBα were repressed by zld1039 (Fig. 10n, o–r). These results suggest that zld1039 may regulate p65 and p-p65 through repressing EZH2independent RKIP upregulation.

DISCUSSIONS

In this study, we identified that a potent and highly selective EZH2 small-molecule inhibitor zld1039, could effectively improve kidney dysfunction, inflammation, and apoptosis through EZH2 inhibition-dependent mechanism. Pharmacologic EZH2 inhibition upregulated RKIP and blocked NF-κB p65 activation to inhibit inflammation. Interestingly, RKIP is knockdown by siRNA method, and zld1039 cannot upregulate RKIP, but the inflammatory response is also inhibited by zld1039, suggesting that upregulation of RKIP was partially involved in the anti-inflammatory effect of zld1039.

Nephrotoxicity is one of the most significant side effects of cisplatin chemotherapy [32]. Multiple pathophysiological mechanisms are involved in cisplatin-induced AKI, including kidney inflammation, cell apoptosis, oxidative stress, proximal tubular injury, and vascular injury [33]. Among them, inflammation involving various cytokines and chemokines, including MCP-1, TNFα, IL-1β, and IL-6, plays crucial roles [34]. Our results revealed that cisplatin triggered inflammatory responses, and inhibiting EZH2 by zld1039 alleviated these corresponding changes. Additionally, cell apoptosis has been considered as one of the main manifestations of renal tubular injury and caspase 3 activation accelerated cisplatin-induced cell death [35]. In the study, we also observed that cisplatin activated caspase 3 expression and induced renal tubular cell apoptosis in injured kidneys. Selective EZH2 inhibition by zld1039 suppressed cisplatin-induced cleaved caspase 3 expression and tubule cell apoptosis. Thus, these data provided strong evidence that pharmacological EZH2 inhibition by zld1039 protected against cisplatin-induced AKI by inhibiting kidney inflammation and tubular cell apoptosis.

EZH2, a core component of PRC2 [36], is responsible for catalyzing H3K27me3 which is an important form of EZH2 enzyme activity and has a transcriptional silencing effect [37].

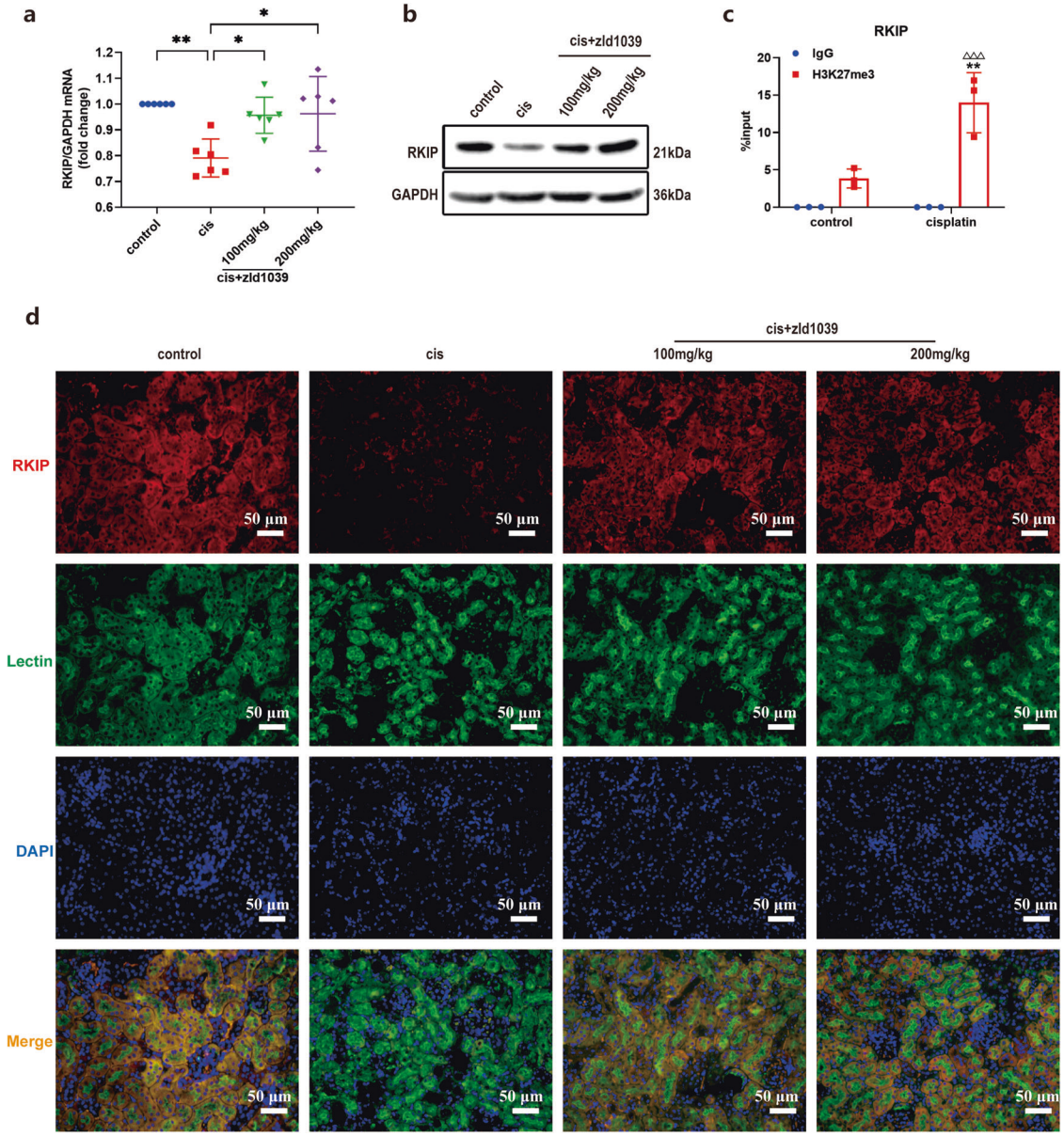

Fig. 5 EZH2 inhibition by zld1039 preserved the expression of RKIP in cisplatin-induced AKI mice. a The mRNA level of RKIP ($n = 6$). $^{**}P < 0.01$, $^{*}P < 0.05$. **b** Protein expression level of RKIP. **c** Control and cisplatin mice kidney tissues were subjected to ChIP assays using immunoglobulin G (IgG) and the H3K27me3 antibody. The amounts of precipitated RKIP DNA were quantified by qPCR using primers amplifying the regions indicated in Table S2. The data are presented as mean ± SD ($n = 3$). $^{**}P < 0.01$ compared with the cisplatin group IgG antibody. $^{\triangle\triangle\triangle}P < 0.001$ compared with the control group H3K27me3 antibody. **d** Photomicrographs (×200) illustrate RKIP immunofluorescence staining of kidney tissues from control or 20 mg/kg cisplatin-treated mice with/without zld1039 administration. All Western blot analyses were performed in two randomized mice from each group, and the experiments were repeated in triplicate.

Overexpression of EZH2 is a biomarker in cancers, and it is intimately correlated with tumor invasiveness and poor prognosis [38, 39]. Apart from tumors, EZH2 is also an essential mediator of different kidney diseases, including AKI [14], hyperuricemic nephropathy [24], and renal fibrosis [23]. As an efficient and selective EZH2 inhibitor, compound zld1039 has been developed to inhibit breast cancer cell growth, induce apoptosis and suppress tumor metastasis via blocking H3K27me3, rather than H3K4me2/3 and H3K9me3 [25]. However, the role of zld1039 as a drug candidate for AKI treatment remains unknown. In this study, pharmacological blockage of EZH2 with zld1039 improved kidney functions in cisplatin-induced AKI. Moreover, our results displayed that cisplatin obviously enhanced EZH2 and H3K27me3, and zld1039 not only inhibited EZH2 methyltransferase activity, but also repressed the expression of EZH2. Furthermore, zld1039 dose-dependently inhibited H3K27me3 in vivo and in vitro, although this dose-dependent effect applied for EZH2 only in vivo. Additionally, zld1039 (1.6 μM) repressed H3K27me3, rather than EZH2 in TCMK-1 cells without cisplatin. These results suggested that zld1039 was mainly responsible for inhibiting EZH2 methyltransferase activity in a dose-dependent manner and inhibiting overexpression of EZH2, but had no effect on normal EZH2.

NF-κB as a transcription factor regulates the expression of pro-inflammatory cytokines/chemokines, and also participates in cell apoptosis, proliferation, and differentiation [40, 41]. Previously, Ozkok et al. have shown that NF-κB inhibitor JSH-23 decreased pro-inflammatory mediators by directly suppressing NF-κB transcriptional activity, and ameliorated cisplatin-induced AKI [42]. Our

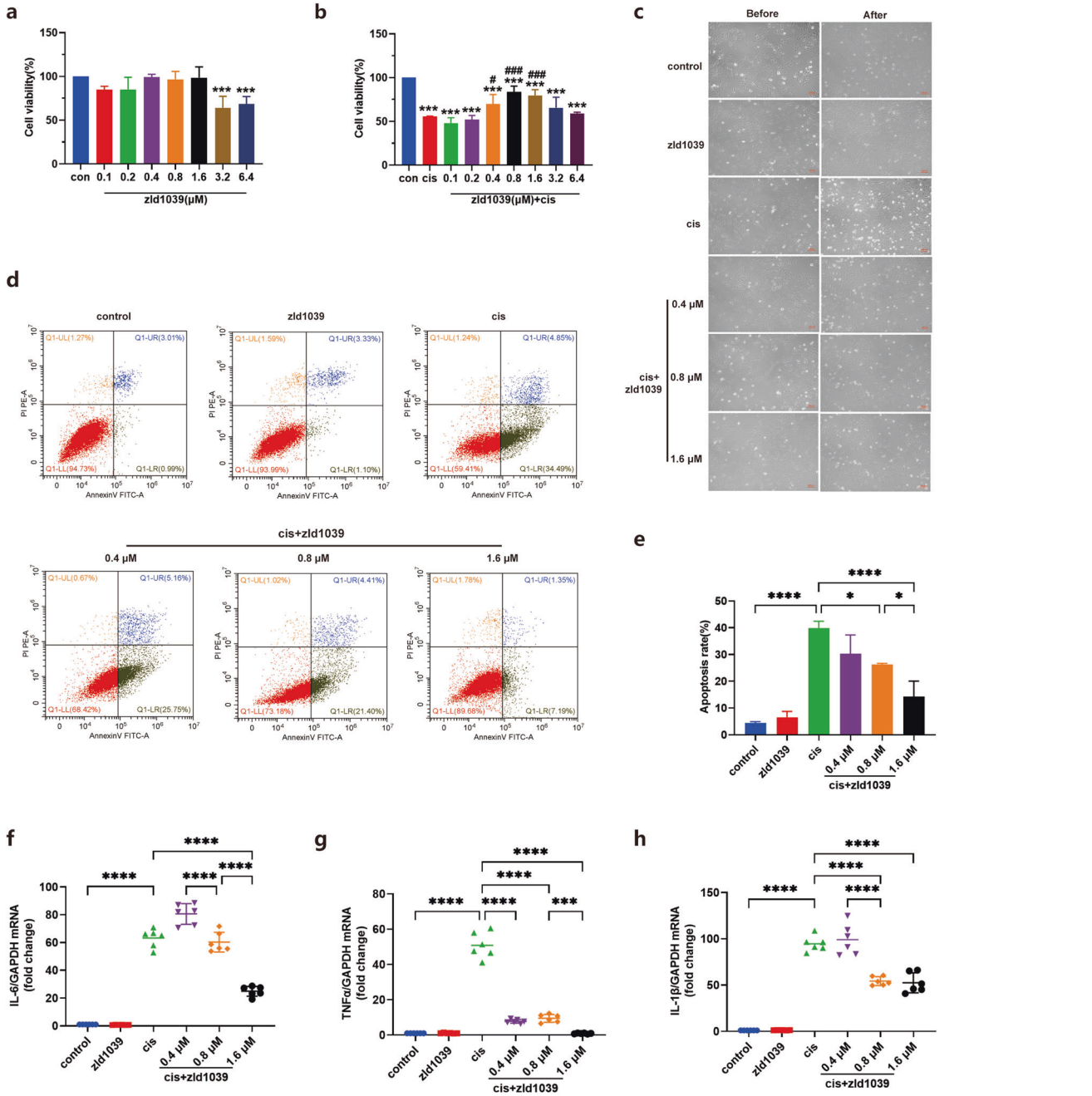

Fig. 6 EZH2 inhibition by zld1039 alleviated cisplatin-induced mouse renal tubular epithelial cells apoptosis and inflammation. a, **b** Effect of zld1039 at the indicated concentrations on the viability of TCMK-1 cells in the absence or presence of cisplatin as determined by an CCK8 assay. ***$P < 0.001$ compared with the control group. ###$P < 0.001$, #$P < 0.05$ compared with the cis group. **c** Cell damage under light microscope (magnification ×200). **d**, **e** Flow-cytometric analysis of PI/Annexin V-stained TCMK-1 cells and apoptosis rate (%). **f**–**h** The mRNA levels of IL-6, TNFα and IL-1β ****$P < 0.0001$, ***$P < 0.001$, *$P < 0.05$.

data also confirmed that NF-κB p65 pathway was activated following cisplatin injection, and the transcriptional activity of NF-κB could be inhibited by zld1039. Not only, the total p65 expression was also suppressed. That is, cisplatin stimulates the expression of EZH2 and H3K27me3, and the total p65 expression in the injured kidneys is increased. How does EZH2 and H3K27me3 upregulate the total p65 level? We discovered that under normal circumstances, H3K27me3 was observably bound to the p65 (Rela) promoter regions, while cisplatin stimulation inhibited H3K27me3 to bind to these regions. The inhibitory effect of H3K27me3 on p65 transcription was weakened, contributing to the transcriptional upregulation of total p65. Moreover, it is reported that EZH2 directly binds to the promoter of AR gene, accompanied by recruiting transcriptional activator H3K27ac, thereby increasing AR gene expression and accelerating the progression of prostate cancer [18]. Additionally, CHIP-seq data also showed that only EZH2, but not H3K27me3, directly bounds to the AR promoter, which suggests EZH2 may play an activating role by co-existing with H3K27ac independent of PRC2 and its methyltransferase activity [18]. In our cisplatin group of mice, EZH2 was markedly enhanced, accompanied by H3K27ac and total p65 upregulation, indicating that the upregulation of

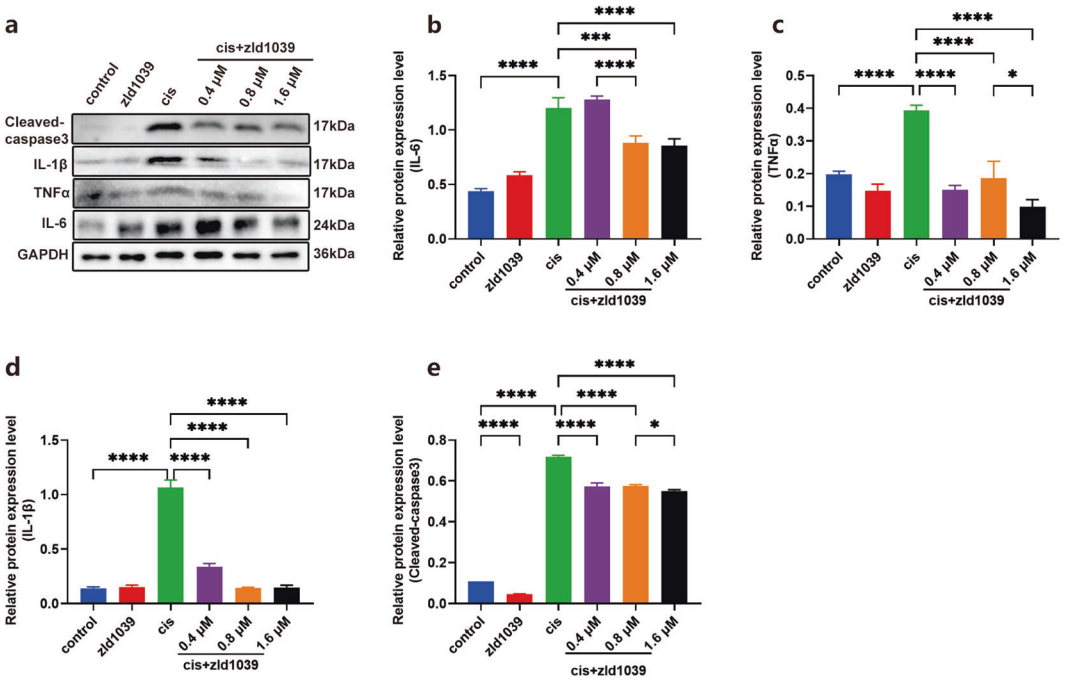

Fig. 7 EZH2 inhibition by zld1039 alleviated cisplatin-induced mouse renal tubular epithelial cells apoptosis and inflammation. **a**–**e** Protein expression levels of cleaved caspase 3, IL-1β, TNFα, and IL-6 were quantified by densitometry and normalized with GAPDH. ****$P < 0.0001$, ***$P < 0.001$, *$P < 0.05$. All Western blot analyses were performed in triplicate.

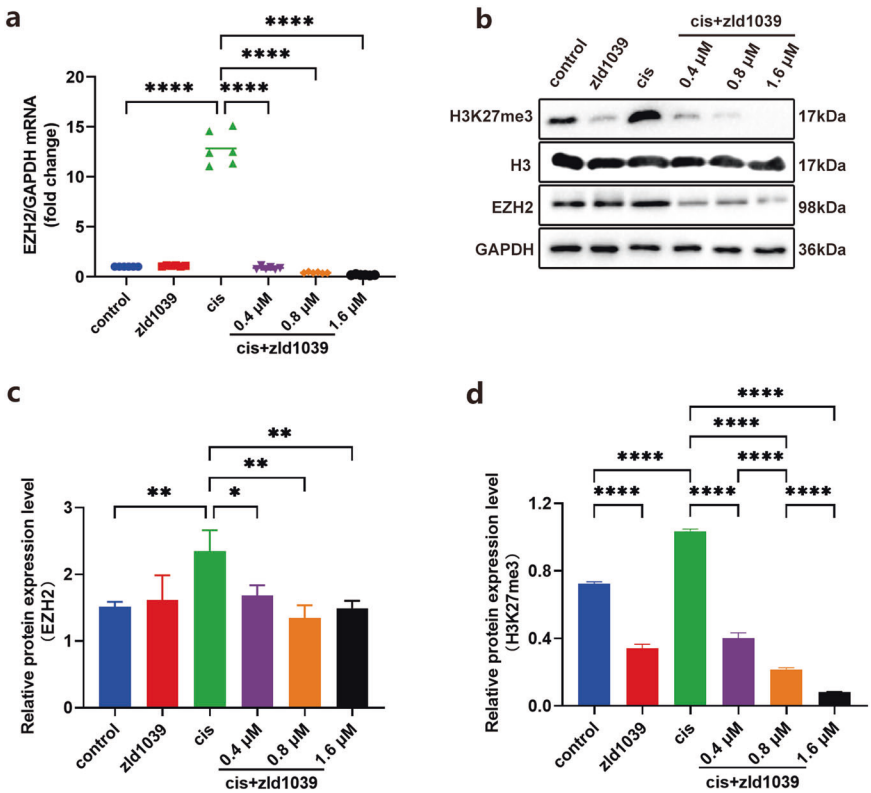

Fig. 8 EZH2 inhibition by zld1039 inhibited cisplatin-induced tubular cell apoptosis and inflammation by H3K27me3-dependent manner. **a** The mRNA level of EZH2. **b**–**d** Protein expression levels of EZH2 and H3K27me3 were quantified by densitometry and normalized with GAPDH. ****$P < 0.0001$, **$P < 0.01$, *$P < 0.05$. All Western blot analyses were performed in triplicate.

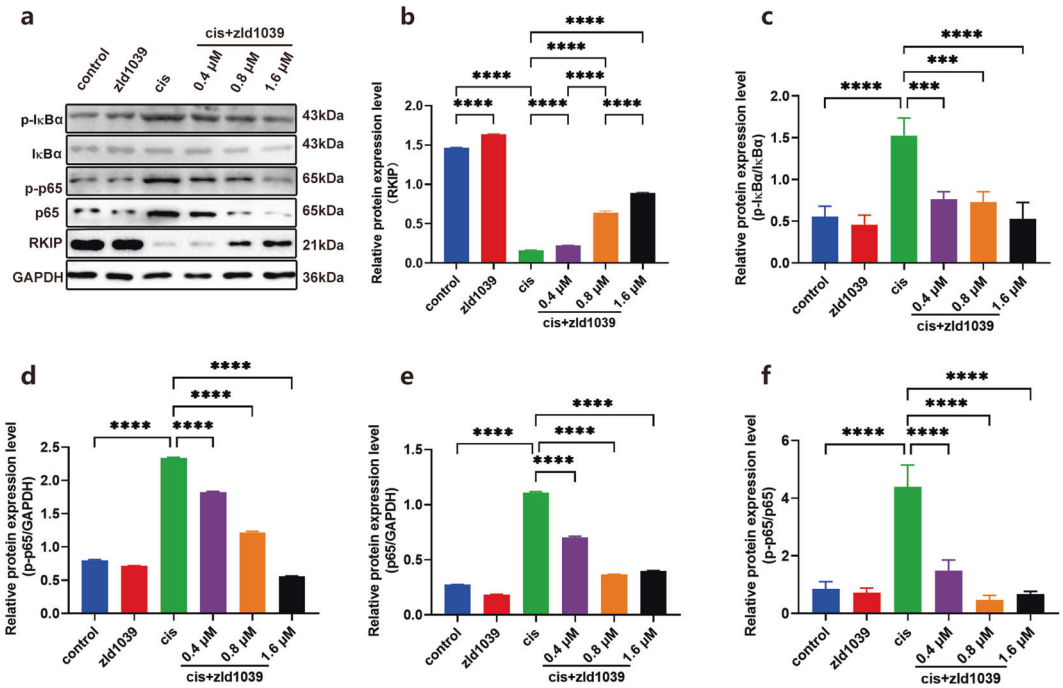

Fig. 9 EZH2 inhibition by zld1039 preserved RKIP expression and inhibited the activation of NF-κB signaling in cisplatin-stimulated TCMK-1 cells. a–f Protein expression levels of RKIP, p65, p-p65, IκBα, and p-IκBα were quantified by densitometry and normalized with GAPDH. $^{****}P < 0.0001$, $^{***}P < 0.001$. All Western blot analyses were performed in triplicate.

total p65 may be partially related to EZH2 recruitment of H3K27ac to activate p65 transcription. EZH2 can play a transcriptional activation role.

RKIP, a small cytoplasmic protein, is a member of the PEBP family [29]. It is involved in cell growth, differentiation, proliferation, apoptosis and modulates various physiological responses through Raf-MEK-MAPK, GPCR, NF-κB pathways, such as mitogenic, inflammation, and stress stimulus [43]. Referring to the classic NF-κB signaling pathway, RKIP physically interacts with IκBα, subsequently represses IκBα phosphorylation and p65 nucleus translocation. RKIP also relieves adhesion molecules expression by decreasing IκBα degradation and inhibiting p65 activation [30]. The deficiency of RKIP has particular effect on inflammatory diseases [44]. For instance, RKIP inhibition accelerates acute liver failure by activating the NF-κB p65 signaling [45]. Given that zld1039 has been demonstrated as a potential epigenetic drug candidate and it might block inflammation by repressing NF-κB p65 signaling pathway. We speculated that RKIP might also play an important role in AKI. As expected, we detected a low level of RKIP and a high level of NF-κB p65 in kidneys of the cisplatin-induced AKI. EZH2 inhibition by zld1039 upregulated RKIP and subsequently downregulated NF-κB p65, indicating that zld1039 targets RKIP that is critical for the NF-κB p65 inhibition. Furthermore, we found that zld1039 could reduce cisplatin-induced inflammatory response in RKIP knockdown cells, although failed to upregulate RKIP expression. Collectively, combined with the results in vivo, EZH2 inhibitor zld1039 indeed successfully rescued the expression of RKIP to exert renal protection, but the upregulation of RKIP is not necessary for zld1039 to exert anti-inflammatory effect in RKIP knockdown cells, which suggests that zld1039 may mediate renal protection partly through upregulation of RKIP, rather than completely dependent on RKIP.

Because zld1039 partially upregulated RKIP expression, what caused the change of NF-κB p65 signaling in RKIP knockdown cells? Recently, non-histone methylation has become increasingly important in regulating cellular pathways. Non-histone methylation is also involved in translational and posttranslational regulation of gene expression. Although methylases are histone specific, many have been found to modify both histone and non-histone substrates. EZH2 also methylates various transcription factors including AR, GATA-binding protein 4, and retinoic acid-related-orphan receptors (RORα), other than histone H3 [46, 47]. EZH2 methylates STAT3 at K180, which further promotes STAT3 transcriptional activity and promotes glioblastoma and prostate cancer progression [47]. Similarly, we found that EZH2 increased p65 transcriptional activity after cisplatin stimulation, which was repressed by zld1039 in RKIP knockdown cells. There is frequent crosstalk between methylation and other types of posttranslational modifications, such as phosphorylation and ubiquitination [48]. In human non-histones, over 60% of the methylated residues are within the ten amino acids range of the phosphorylation site [49]. It is possible that EZH2 promotes non-histone p65 methylation, and that may directly stimulate p65 phosphorylated activation and enhance p65 transcriptional activity, while zld1039 directly blocks p65 methylation and phosphorylated activation by EZH2 inhibition independent of RKIP. There are far more non-histone substrates than histone substrates, suggesting that methylation has gone far beyond modifying histones. Further investigation about the relationship between p65 methylation and phosphorylated activation is needed. Additionally, in ER-negative basal-like breast cancer cells, EZH2 activates NF-κB signaling and promotes the expression of NF-κB target genes through complexing with RelA and RelB, which is independent of EZH2 histone methyltransferase activity [50]. Zld1039 may block the formation of the EZH2/RelA/RelB complex to directly inhibit NF-κB pathways and inflammatory response in RKIP knockdown cells. Zld1039 can not only target RKIP upregulation by inhibiting H3K27me3, but also directly target non-histone p65 methylation, both of which can regulate NF-κB p65 transcriptional activity. Indeed, the relationship between EZH2 and NF-κB p65 is even more complicated, which will be further explored in our following studies.

EZH2 and H3K27me3 recruits to the RKIP (pebp1) promoter forms a H3K27me3 repressive chromatin structure, and the

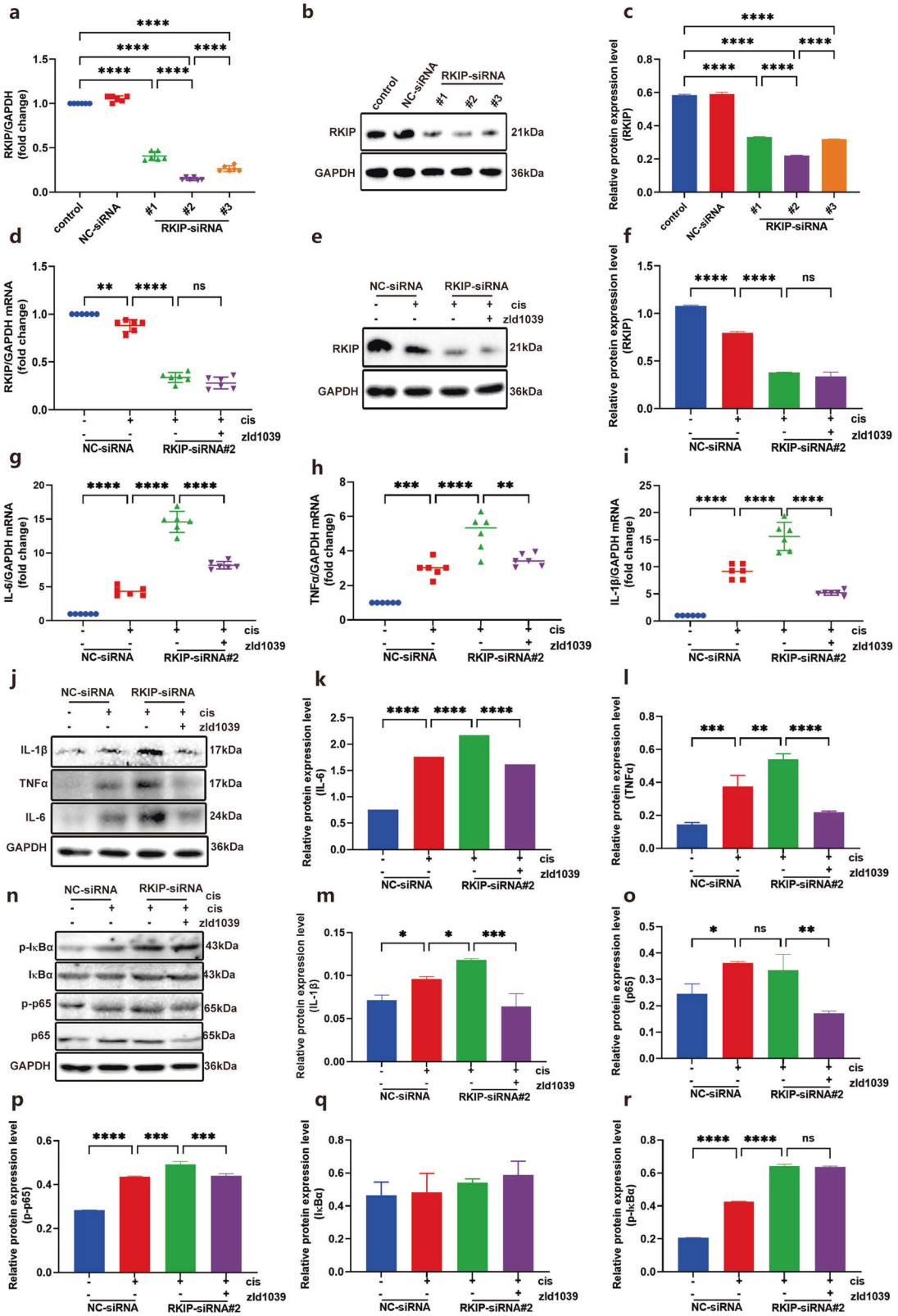

Fig. 10 Effect of RKIP knockdown on inflammation in cisplatin-stimulated TCMK-1 cells. a–c Screening for suitable RKIP-siRNA through mRNA and protein levels. **d–r** TCMK-1 cells were subjected to RKIP knockdown (RKIP-siRNA#2) and then exposed to cisplatin with or without zld1039. Cell lysates were then collected and analyzed by qRT-PCR (**d**, **g–i**) or Western blotting (**e**, **j**, **n**). $^{****}P < 0.0001$, $^{***}P < 0.001$, $^{**}P < 0.01$, $^{*}P < 0.05$, $^{ns}P > 0.05$. All Western blot analyses were performed in triplicate.

expression of RKIP is inhibited [51, 52]. In our study, we observed that cisplatin increased EZH2 and H3K27me3 and decreased RKIP expression. In contrast, oral administration of EZH2 inhibitor zld1039 reduced EZH2 and H3K27me3 and preserved RKIP, suggesting that EZH2 and H3K27me3 may be a regulator of RKIP in kidneys of cisplatin-induced AKI. To explore whether EZH2 and H3K27me3 have physical interaction with the RKIP (pebp1) promoter in cisplatin-induced AKI mice, we further used the CHIP assay for verification. We found that H3K27me3 could directly bind to the RKIP (pebp1) promoter region, the level of H3K27me3 on the RKIP (pebp1) promoter in the kidneys of mice in cisplatin group was higher than that of control mice. That is, the enrichment of H3K27me3 and RKIP (pebp1) promoter inhibits the expression of RKIP. Surprisingly, there was very few enrichments between EZH2 and the RKIP (pebp1) promoter, This result contradicts what Ren et al. have reported in breast and prostate cancer cells, in which EZH2 repressed RKIP expression via physically binding to the RKIP (pebp1) promoter [20]. The reason for this discrepancy may be the fact that CHIP-seq data of EZH2 were derived from non-renal cells, resulting in weakened applicability of the data in renal tissues. The conclusion is that H3K27me3 rather than EZH2 itself exerts the inhibitory effect on RKIP transcription, but H3K27me3 must depend on EZH2 methyltransferase activity.

In summary, this is the first study to verify that novel EZH2 inhibitor zld1039 alleviated cisplatin-induced kidney inflammation and cell apoptosis. Notably, EZH2-regulated histone modification H3K27me3 are indeed involved in transcriptional inhibition of renal protective gene RKIP. Pharmacologic EZH2 inhibition by zld1039 inhibited NF-κB p65 signaling by suppressing EZH2 and enhancing RKIP expression. Consequently, our study provided a comprehensive mechanism by which EZH2 inhibition alleviated renal inflammation and cell apoptosis partially via RKIP and NF-κB p65 pathway in cisplatin-induced AKI. The potent and highly selective EZH2 inhibitor zld1039 may serve as a promising treatment for AKI.

ACKNOWLEDGEMENTS

This study was supported by the National Key R&D Program of China (2020YFC2005000), the National Natural Science Foundation of China (82070711), the Science/Technology Project of Sichuan province (2020YFQ0055), and the 1.3.5 project for disciplines of excellence from West China Hospital of Sichuan University (ZYGD18027).

AUTHOR CONTRIBUTIONS

LW, LDZ, and LM designed research, analyzed data, and drafted the article; FG, SHT, and PF contributed new reagents or analytic tools; LZL analyzed and interpretated data; HLY performed research; YL analyzed data; All authors finally approved the version to be published.

ADDITIONAL INFORMATION

Supplementary information The online version contains supplementary material available at https://doi.org/10.1038/s41401-021-00837-8.

Competing interests: The authors declare no competing interests.

REFERENCES

1. Coelho S, Cabral G, Lopes JA, Jacinto A. Renal regeneration after acute kidney injury. Nephrology. 2018;23:805–14.
2. Guo C, Dong G, Liang X, Dong Z. Epigenetic regulation in AKI and kidney repair: mechanisms and therapeutic implications. Nat Rev Nephrol. 2019;15:220–39.
3. Ronco C, Bellomo R, Kellum JA. Acute kidney injury. Lancet. 2019;394:1949–64.
4. Fu Y, Tang C, Cai J, Chen G, Zhang D, Dong Z. Rodent models of AKI-CKD transition. Am J Physiol Ren Physiol. 2018;315:F1098–F1106.
5. Wen X, Murugan R, Peng Z, Kellum JA. Pathophysiology of acute kidney injury: a new perspective. Contrib Nephrol. 2010;165:39–45.
6. Lameire NH, Bagga A, Cruz D, De Maeseneer J, Endre Z, Kellum JA, et al. Acute kidney injury: an increasing global concern. Lancet. 2013;382:170–9.
7. Siddik ZH. Cisplatin: mode of cytotoxic action and molecular basis of resistance. Oncogene. 2003;22:7265–79.
8. Tanase DM, Gosav EM, Radu S, Costea CF, Ciocoiu M, Carauleanu A, et al. The predictive role of the biomarker kidney molecule-1 (KIM-1) in acute kidney injury (AKI) cisplatin-induced nephrotoxicity. Int J Mol Sci. 2019;20:5238.
9. Sánchez-González PD, López-Hernández FJ, López-Novoa JM, Morales AI. An integrative view of the pathophysiological events leading to cisplatin nephrotoxicity. Crit Rev Toxicol. 2011;41:803–21.
10. Bolisetty S, Traylor A, Joseph R, Zarjou A, Agarwal A. Proximal tubule-targeted heme oxygenase-1 in cisplatin-induced acute kidney injury. Am J Physiol Ren Physiol. 2015;310:F385–F394.
11. Zhu S, Pabla N, Tang C, He L, Dong Z. DNA damage response in cisplatin-induced nephrotoxicity. Arch Toxicol. 2015;89:2197–205.
12. Xu Y, Ma H, Shao J, Wu J, Zhou L, Zhang Z, et al. A role for tubular necroptosis in cisplatin-induced AKI. J Am Soc Nephrol. 2015;26:2647.
13. Zhou X, Zang X, Guan Y, Tolbert T, Zhao TC, Bayliss G, et al. Targeting enhancer of zeste homolog 2 protects against acute kidney injury. Cell Death Dis. 2018;9:1067.
14. Ni J, Hou X, Wang X, Shi Y, Xu L, Zheng X, et al. 3-deazaneplanocin A protects against cisplatin-induced renal tubular cell apoptosis and acute kidney injury by restoration of E-cadherin expression. Cell Death Dis. 2019;10:355.
15. Liu X, Wu Q, Li L. Functional and therapeutic significance of EZH2 in urological cancers. Oncotarget. 2017;8:38044–55.
16. Kim KH, Roberts CWM. Targeting EZH2 in cancer. Nat Med. 2016;22:128–34.
17. Hanaki S, Shimada M. Targeting EZH2 as cancer therapy. J Biochem. 2021;170:1–4.
18. Kim J, Lee Y, Lu X, Song B, Fong K-W, Cao Q, et al. Polycomb- and methylation-independent roles of EZH2 as a transcription activator. Cell Rep. 2018;25:2808–.e2804.
19. Nie L, Wei Y, Zhang F, Hsu Y-H, Chan L-C, Xia W, et al. CDK2-mediated site-specific phosphorylation of EZH2 drives and maintains triple-negative breast cancer. Nat Commun. 2019;10:5114.
20. Ren G, Baritaki S, Marathe H, Feng J, Park S, Beach S, et al. Polycomb protein EZH2 regulates tumor invasion via the transcriptional repression of the metastasis suppressor RKIP in breast and prostate cancer. Cancer Res. 2012;72:3091.
21. Xu Y, Wang H, Li F, Heindl LM, He X, Yu J, et al. Long Non-coding RNA LINC-PINT Suppresses Cell Proliferation and Migration of Melanoma via Recruiting EZH2. Front Cell Dev Biol. 2019;7:350.
22. Ramakrishnan S, Granger V, Rak M, Hu Q, Attwood K, Aquila L, et al. Inhibition of EZH2 induces NK cell-mediated differentiation and death in muscle-invasive bladder cancer. Cell Death Differ. 2019;26:2100–14.
23. Zhou X, Xiong C, Tolbert E, Zhao TC, Bayliss G, Zhuang S. Targeting histone methyltransferase enhancer of zeste homolog-2 inhibits renal epithelial-mesenchymal transition and attenuates renal fibrosis. FASEB J. 2018;32:5976–89.
24. Shi Y, Xu L, Tao M, Fang L, Lu J, Gu H, et al. Blockade of enhancer of zeste homolog 2 alleviates renal injury associated with hyperuricemia. Am J Physiol Ren Physiol. 2018;316:F488–F505.
25. Song X, Gao T, Wang N, Feng Q, You X, Ye T, et al. Correction: Corrigendum: Selective inhibition of EZH2 by ZLD1039 blocks H3K27methylation and leads to potent anti-tumor activity in breast cancer. Sci Rep. 2016;6:24893.
26. Sato Y, Yanagita M. Immune cells and inflammation in AKI to CKD progression. Am J Physiol Ren Physiol. 2018;315:F1501–F1512.
27. Zhang X, Wang Y, Yuan J, Li N, Pei S, Xu J, et al. Macrophage/microglial Ezh2 facilitates autoimmune inflammation through inhibition of Socs3. J Exp Med. 2018;215:1365–82.
28. Mu W, Starmer J, Fedoriw AM, Yee D, Magnuson T. Repression of the soma-specific transcriptome by Polycomb-repressive complex 2 promotes male germ cell development. Genes Dev. 2014;28:2056–69.
29. Caltabiano R, Puzzo L, Barresi V, Cardile V, Loreto C, Ragusa M, et al. Expression of Raf Kinase Inhibitor Protein (RKIP) is a predictor of uveal melanoma metastasis. Histol Histopathol. 2016;29:1325–34.
30. Jing SH, Gao X, Yu B, Qiao H. Raf kinase inhibitor protein (RKIP) inhibits tumor necrosis factor-α (TNF-α) induced adhesion molecules expression in vascular smooth muscle bells by suppressing (nuclear transcription factor-κB (NF-kappaB) pathway. Med Sci Monitor. 2017;23:4789–97.
31. Späth MR, Bartram MP, Palacio-Escat N, Hoyer KJR, Debes C, Demir F, et al. The proteome microenvironment determines the protective effect of preconditioning in cisplatin-induced acute kidney injury. Kidney Int. 2019;95:333–49.
32. Shiraishi F, Curtis LM, Truong L, Poss K, Visner GA, Madsen K, et al. Heme oxygenase-1 gene ablation or expression modulates cisplatin-induced renal tubular apoptosis. Am J Physiol Ren Physiol. 2000;278:F726–F736.
33. Ozkok A, Edelstein CL. Pathophysiology of cisplatin-induced acute kidney injury. BioMed Res Int. 2014;2014:967826.

34. Faubel S, Lewis EC, Reznikov L, Ljubanovic D, Hoke TS, Somerset H, et al. Cisplatin-induced acute renal failure is associated with an increase in the cytokines interleukin (IL)-1β, IL-18, IL-6, and neutrophil infiltration in the kidney. J Pharmacol Exp Ther. 2007;322:8–15.
35. Herzog C, Yang C, Holmes A, Kaushal GP. zVAD-fmk prevents cisplatin-induced cleavage of autophagy proteins but impairs autophagic flux and worsens renal function. Am J Physiol Ren Physiol. 2012;303:F1239–F1250.
36. Schuettengruber B, Chourrout D, Vervoort M, Leblanc B, Cavalli G. Genome regulation by polycomb and trithorax proteins. Cell. 2007;128:735–45.
37. Sauvageau M, Sauvageau G. Polycomb group proteins: multi-faceted regulators of somatic stem cells and cancer. Cell Stem Cell. 2010;7:299–313.
38. Gong Y, Huo L, Liu P, Sneige N, Sun X, Ueno NT, et al. Polycomb group protein EZH2 is frequently expressed in inflammatory breast cancer and is predictive of worse clinical outcome. Cancer. 2011;117:5476–84.
39. Collett K, Eide GE, Arnes J, Stefansson IM, Eide J, Braaten A, et al. Expression of enhancer of zeste homologue 2 is significantly associated with increased tumor cell proliferation and is a marker of aggressive breast cancer. Clin Cancer Res. 2006;12:1168–74.
40. Perkins ND. Integrating cell-signalling pathways with NF-κB and IKK function. Nat Rev Mol Cell Biol. 2007;8:49–62.
41. Basak S, Hoffmann A. Crosstalk via the NF-kappaB signaling system. Cytokine Growth Factor Rev. 2008;19:187–97.
42. Ozkok A, Ravichandran K, Wang Q, Ljubanovic D, Edelstein CL. NF-κB transcriptional inhibition ameliorates cisplatin-induced acute kidney injury (AKI). Toxicol Lett. 2016;240:105–13.
43. Zeng L, Imamoto A, Rosner MR. Raf kinase inhibitory protein (RKIP): a physiological regulator and future therapeutic target. Expert Opin Ther Targets. 2008;12:1275–87.
44. Qin Q, Liu H, Shou J, Jiang Y, Yu H, Wang X. The inhibitor effect of RKIP on inflammasome activation and inflammasome-dependent diseases. Cell Mol Immunol. 2021;18:992–1004.
45. Lin X, Wei J, Nie J, Bai F, Zhu X, Zhuo L, et al. Inhibition of RKIP aggravates thioacetamide-induced acute liver failure in mice. Exp Ther Med. 2018;16:2992–8.
46. He A, Shen X, Ma Q, Cao J, von Gise A, Zhou P, et al. PRC2 directly methylates GATA4 and represses its transcriptional activity. Genes Dev. 2012;26:37–42.
47. Kim E, Kim M, Woo D-H, Shin Y, Shin J, Chang N, et al. Phosphorylation of EZH2 activates STAT3 signaling via STAT3 methylation and promotes tumorigenicity of glioblastoma stem-like cells. Cancer Cell. 2013;23:839–52.
48. Biggar KK, Li SSC. Non-histone protein methylation as a regulator of cellular signalling and function. Nat Rev Mol Cell Biol. 2015;16:5–17.
49. Hornbeck PV, Zhang B, Murray B, Kornhauser JM, Latham V, Skrzypek E. PhosphoSitePlus, 2014: mutations, PTMs and recalibrations. Nucleic Acids Res. 2015;43:D512–520.
50. Lee Shuet T, Li Z, Wu Z, Aau M, Guan P, Karuturi RKM, et al. Context-specific regulation of NF-κB target gene expression by EZH2 in breast cancers. Mol Cell. 2011;43:798–810.
51. Shen H, Laird PW. Interplay between the cancer genome and epigenome. Cell. 2013;153:38–55.
52. Wagener N, Macher-Goeppinger S, Pritsch M, Hüsing J, Hoppe-Seyler K, Schirmacher P, et al. Enhancer of zeste homolog 2 (EZH2) expression is an independent prognostic factor in renal cell carcinoma. BMC Cancer. 2010;10:524.